

# Gaussian Process-Based Prediction and Control of Hammerstein-Wiener Systems

Mingzhou Yin and Matthias A. Müller

**Abstract**—This work investigates data-driven prediction and control of Hammerstein-Wiener systems using physics-informed Gaussian process models. Data-driven prediction algorithms have been developed for structured nonlinear systems based on Willems’ fundamental lemma. However, existing frameworks cannot treat output nonlinearities and require a dictionary of basis functions for Hammerstein systems. In this work, an implicit predictor structure is considered, leveraging the multi-step-ahead ARX structure for the linear part of the model. This implicit function is learned by Gaussian process regression with kernel functions designed from Gaussian process priors for the nonlinearities. The linear model parameters are estimated as hyperparameters by assuming a stable spline hyperprior. The implicit Gaussian process model provides explicit output prediction by optimizing selected optimality criteria. The model is also applied to receding horizon control with the expected control cost and chance constraint satisfaction guarantee. Numerical results demonstrate that the proposed prediction and control algorithms are superior to black-box Gaussian process models.

**Index Terms**—Data-driven control, Gaussian processes, nonlinear systems.

## I. INTRODUCTION

In recent years, the problem of data-driven prediction has drawn significant attention due to the emergence of more complex systems and the availability of big data. This problem aims to obtain nonparametric predictors directly from collected input-output data using minimal model knowledge of the system. In this way, model-based predictive controllers can be readily adapted into data-driven ones by employing data-driven predictors. This work investigates data-driven prediction and control of Hammerstein-Wiener systems. Hammerstein-Wiener systems are nonlinear block-oriented models with static input and output nonlinearities, which have a wide range of applications (see [1] and references therein).

Data-driven prediction can be seen as finding a mapping from inputs and initial conditions to outputs, where any function approximators can be applied to learn the mapping. In this regard, a basis function decomposition approach is used in [2]. Gaussian process/kernel regression has been widely used in system identification to estimate the model [3], [4] by designing kernel structures for stable nonlinear systems

inspired by system theory [5]. Kernel-based identification for Hammerstein and Wiener systems is investigated separately in [6], [7] for one-step-ahead prediction. This idea of using system-theoretic knowledge such as model structure in learning is sometimes known as physics-informed approaches [8]. Predictions from the Gaussian process model can then be used in receding horizon control. This approach is referred to as Gaussian process model predictive control [9]–[11].

On the other hand, following the seminal result in [12], known as Willems’ fundamental lemma, data-driven prediction of linear systems has been widely studied by finding suitable linear combinations of collected data, subject to input and initial condition constraints [13]. The predictor can be reformulated as a multi-step-ahead ARX structure. Applying the predictor to receding horizon control leads to data-driven or data-enabled predictive control, for which multiple successful algorithms have been proposed, e.g., [14]–[18].

Extensions of these linear algorithms to nonlinear systems have been analyzed for specific nonlinear model classes, including Hammerstein systems [19], [20], second-order Volterra systems [21], feedback linearizable systems [22], bilinear systems [23], [24], and systems with finite-dimensional Koopman embedding [25]. These extensions generalize Willems’ fundamental lemma by applying generalized signal embedding to the signal matrix and the persistency of excitation condition. This is possibly achieved by assuming a known dictionary of basis functions. However, for Hammerstein-Wiener systems, existing works [19], [24] address only the input nonlinearity (the Hammerstein part) and require prior knowledge of basis functions for the nonlinearity, which is often impractical.

In this work, data-driven prediction of Hammerstein-Wiener systems is first formulated as an implicit function learning problem by considering the multi-step-ahead ARX structure for the linear part. Instead of considering a basis function decomposition as in [2], [19], [20], Gaussian process priors are assumed for the nonlinearities and the kernel functions for the implicit prediction model are derived. The implicit Gaussian process model [26] then provides posterior predictions by optimizing selected optimality criteria, such as maximum likelihood. The linear model parameters act as hyperparameters in the Gaussian process model, which are estimated by enforcing a stable spline hyperprior to avoid overfitting [3], [4]. The nonlinearities can also be recovered separately using additional Gaussian process regression procedures. The implicit Gaussian process prediction is applied to receding horizon control by considering the expected control cost and guaranteeing output chance constraint satisfaction. Finally, the predictor and the control algorithm are verified in numerical examples and

The authors are with the Institute of Automatic Control, Leibniz University Hannover, 30167 Hannover, Germany (e-mail: yin@irt.uni-hannover.de; mueller@irt.uni-hannover.de).

This work was supported by the Lower Saxony Ministry for Science and Culture within the program *zukunf.niedersachsen*.

© 2025 IEEE. Personal use of this material is permitted. Permission from IEEE must be obtained for all other uses, in any current or future media, including reprinting/republishing this material for advertising or promotional purposes, creating new collective works, for resale or redistribution to servers or lists, or reuse of any copyrighted component of this work in other works.

demonstrate better performance than the linear predictor and the black-box Gaussian process predictor with a nonlinear ARX model.

The remainder of the paper is organized as follows. Section II introduces the problem and presents the implicit predictor structure. Section III proposes the data-driven prediction algorithm by Gaussian process regression. Section IV applies the data-driven predictor to receding horizon control, followed by numerical examples in Section V. Section VI concludes the paper.

*Notation.* The expected value and covariance of a random variable are denoted by  $\mathbb{E}[\cdot]$  and  $\text{cov}(\cdot)$ , respectively. The symbol  $\text{Pr}(\cdot)$  indicates the probability of a random event. For a sequence of matrices  $X_1, \dots, X_n$ , we denote the row-wise and diagonal-wise concatenation by  $\text{col}(X_1, \dots, X_n)$  and  $\text{blkdiag}(X_1, \dots, X_n)$ , respectively. Given a signal  $x : \{1, \dots, N\} \rightarrow \mathbb{R}^n$ , the Hankel matrix of depth  $L$  is defined as

$$\mathcal{H}_L(\mathbf{x}) = \begin{bmatrix} x_1 & x_2 & \cdots & x_{N-L+1} \\ x_2 & x_3 & \cdots & x_{N-L+2} \\ \vdots & \vdots & \ddots & \vdots \\ x_L & x_{L+1} & \cdots & x_N \end{bmatrix},$$

and its trajectory from  $i$  to  $j$  is indicated by  $(x_k)_{k=i}^j = \text{col}(x_i, \dots, x_j)$ . For a vector  $x$ ,  $\|x\|_P$  denotes the weighted  $l_2$ -norm  $(x^\top P x)^{\frac{1}{2}}$ . The trace, log-determinant, and column vector containing the diagonal elements of a square matrix are indicated by  $\text{tr}(\cdot)$ ,  $\text{logdet}(\cdot)$ , and  $\text{diag}(\cdot)$ , respectively. The vectorization of a matrix is denoted by  $\text{vec}(\cdot)$ . The symbols  $\otimes$  and  $\dagger$  denote the Kronecker product and the Moore–Penrose inverse, respectively.

## II. PROBLEM STATEMENT AND BACKGROUND

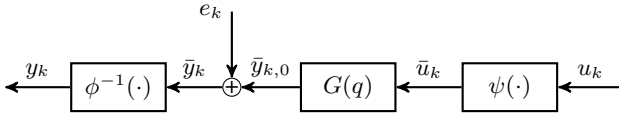


Fig. 1. Block diagram of Hammerstein-Wiener systems.

Consider a Hammerstein-Wiener system shown in Fig. 1, given by

$$\begin{cases} x_{k+1} = Ax_k + B\bar{u}_k, & \bar{u}_k = \psi(u_k), \\ \bar{y}_k = Cx_k + D\bar{u}_k + e_k, & y_k = \phi^{-1}(\bar{y}_k), \end{cases} \quad (1)$$

where  $x_k \in \mathbb{R}^{n_x}$ ,  $u_k \in \mathbb{R}^{n_u}$ ,  $y_k \in \mathbb{R}^{n_y}$  are the states, inputs, and outputs, respectively. The linear part of the system is denoted by  $G(q)$ , where  $\bar{u}_k \in \mathbb{R}^{n_u}$ ,  $\bar{y}_{k,0} \in \mathbb{R}^{n_y}$ ,  $\bar{y}_k \in \mathbb{R}^{n_y}$ ,  $e_k \in \mathbb{R}^{n_y}$  are the inputs, noise-free outputs, outputs, and output noise of  $G(q)$ , respectively. Functions  $\psi(\cdot) : \mathbb{R}^{n_u} \rightarrow \mathbb{R}^{n_u}$ ,  $\phi^{-1}(\cdot) : \mathbb{R}^{n_y} \rightarrow \mathbb{R}^{n_y}$  denote the input and output nonlinearities, respectively.

In this paper, the following assumption is considered.

*Assumption 1:* 1) The output noise  $e_k \in \mathbb{R}^{n_y}$  is zero-mean i.i.d. Gaussian with covariance  $\sigma^2 \mathbb{I}$ , 2) the linear part of the system  $G(q)$  is stable, and 3)  $\phi^{-1}(\cdot)$  is bijective.

*Remark 1:* The model is ambiguous up to scaling factors, i.e., the model triplet  $(\psi(\cdot), G(q), \phi^{-1}(\cdot))$  is equivalent to  $(a\psi(\cdot), \frac{1}{ab}G(q), b\phi^{-1}(\cdot))$ ,  $a, b \in \mathbb{R}$ . Thus, the nonlinearities  $\psi(\cdot)$  and  $\phi(\cdot)$  are normalized during learning in later sections.

In this work, we are interested in characterizing probable length- $L$  input-output trajectory of (1) without model knowledge of  $\psi(\cdot)$ ,  $G(q)$ , and  $\phi^{-1}(\cdot)$ , but from collected input-output trajectory  $(\mathbf{u}^d, \mathbf{y}^d) := (u_k^d, y_k^d)_{k=1}^N$ . This characterization is then used to design a receding horizon control algorithm.

### A. Data-Driven Prediction as Linear Systems

This problem has been widely studied for linear systems, i.e., when  $\psi(\cdot)$  and  $\phi^{-1}(\cdot)$  are known. One successful approach recently relies on Willems' fundamental lemma [12], skipping the explicit step of system identification. In detail, for  $\mathbf{u} = (u_k)_{k=1}^L$  and  $\mathbf{y} = (y_k)_{k=1}^L$ , define  $\Psi(\mathbf{u}) := \text{col}(\psi(u_1), \dots, \psi(u_L))$  and  $\Phi(\mathbf{y}) := \text{col}(\phi(y_1), \dots, \phi(y_L))$ . We have the following lemma.

*Lemma 1:* Suppose  $(\mathbf{u}^d, \mathbf{y}^d) := (u_k^d, y_k^d)_{k=1}^N$  is a noise-free trajectory of the Hammerstein-Wiener system (1). Let  $\bar{\mathbf{u}}^d := \Psi(\mathbf{u}^d)$ ,  $\bar{\mathbf{y}}^d := \Phi(\mathbf{y}^d)$ . If  $\bar{\mathbf{u}}^d$  is persistently exciting of order  $(L + n_x)$ , i.e.,  $\mathcal{H}_{L+n_x}(\bar{\mathbf{u}}^d)$  has full row rank, and  $G(q)$  is controllable,  $(\mathbf{u}, \mathbf{y}) := (u_k, y_k)_{k=1}^L$  is a trajectory of (1) iff there exists  $g \in \mathbb{R}^M$ ,  $M = N - L + 1$ , such that  $\text{col}(H_{\bar{u}}, H_{\bar{y}})g = \text{col}(\bar{\mathbf{u}}, \bar{\mathbf{y}}_0)$ , where  $H_{\bar{u}} := \mathcal{H}_L(\bar{\mathbf{u}}^d)$ ,  $H_{\bar{y}} := \mathcal{H}_L(\bar{\mathbf{y}}^d)$ ,  $\bar{\mathbf{u}} := \Psi(\mathbf{u})$ , and  $\bar{\mathbf{y}}_0 := \Phi(\mathbf{y}) - \mathbf{e}$  denotes the noise-free output of  $G(q)$ , where  $\mathbf{e} := (e_k)_{k=1}^L$ .

*Proof:* This is a direct extension of Willems' fundamental lemma, originally proposed in [12, Theorem 1]. ■

Let  $L = L_0 + L'$ , where  $L_0$  is no smaller than the lag of  $G(q)$ . There exists a mapping from  $\mathbf{u}$  and  $\mathbf{y}_p := (y_k)_{k=1}^{L_0}$  to  $\mathbf{y}_f := (y_k)_{k=L_0+1}^L$ . Define  $\bar{\mathbf{y}}_0 := \text{col}(\bar{\mathbf{y}}_{p,0}, \bar{\mathbf{y}}_{f,0})$  and  $H_{\bar{y}} := \text{col}(H_{\bar{y}p}, H_{\bar{y}f})$ , where  $\bar{\mathbf{y}}_{p,0} \in \mathbb{R}^{n_y L_0}$ ,  $\bar{\mathbf{y}}_{f,0} \in \mathbb{R}^{n_y L'}$ ,  $H_{\bar{y}p} \in \mathbb{R}^{n_y L_0 \times M}$ , and  $H_{\bar{y}f} \in \mathbb{R}^{n_y L' \times M}$ . The mapping can be calculated by  $g = \text{col}(H_{\bar{u}}, H_{\bar{y}p})^\dagger \text{col}(\bar{\mathbf{u}}, \bar{\mathbf{y}}_{p,0})$ ,  $\bar{\mathbf{y}}_{f,0} = H_{\bar{y}f}g$ . This leads to the following corollary.

*Corollary 1:* An input-output sequence  $(\mathbf{u}, \mathbf{y})$  is a trajectory of (1) iff it satisfies

$$\mathbf{0} = [\Gamma_1 \ \Gamma_2 \ -\mathbb{I}] \text{col}(\Psi(\mathbf{u}), \Phi(\mathbf{y}_p), \Phi(\mathbf{y}_f)) + [-\Gamma_2 \ \mathbb{I}] \mathbf{e}. \quad (2)$$

where

$$[\Gamma_1 \ \Gamma_2] := H_{\bar{y}f} \text{col}(H_{\bar{u}}, H_{\bar{y}p})^\dagger \in \mathbb{R}^{n_y L' \times (n_u L + n_y L_0)}. \quad (3)$$

*Proof:* This is a direct extension of the data-driven simulation result, originally proposed in [13, Proposition 1]. ■

*Remark 2:* Equation (2) can be seen as a nonlinear multi-step-ahead ARX model:

$$\mathbf{y}_f = \Phi^{-1}([\Gamma_1 \ \Gamma_2] \text{col}(\Psi(\mathbf{u}), \Phi(\mathbf{y}_p)) + [-\Gamma_2 \ \mathbb{I}] \mathbf{e}).$$

For linear systems, this predictor is known as the subspace predictor [27], and is equivalent to the solution to the least-squares problem [28]:

$$\min_{\Gamma_1, \Gamma_2} \|H_{\bar{y}f} - [\Gamma_1 \ \Gamma_2] \text{col}(H_{\bar{u}}, H_{\bar{y}p})\|_F^2.$$

*Remark 3:* A strategy to analyze Hammerstein-Wiener systems with unknown input and output nonlinearities is to assume that finite-dimensional basis functions are available for the nonlinearities [19], i.e.,  $\psi(\cdot) =: \sum_{i=1}^r a_i \psi_i(\cdot) =: (\mathbf{a}^\top \otimes \mathbb{I}) \psi(\cdot)$ ,  $\phi(\cdot) =: \sum_{i=1}^q b_i \phi_i(\cdot) =: (\mathbf{b}^\top \otimes \mathbb{I}) \phi(\cdot)$ . This leads to

$$\begin{cases} x_{k+1} &= Ax_k + \bar{B}\psi(u_k), \\ (\mathbf{b}^\top \otimes \mathbb{I}) \phi(y_k) &= Cx_k + \bar{D}\psi(u_k), \end{cases} \quad (4)$$

where  $\bar{B} := B(\mathbf{a}^\top \otimes \mathbb{I})$  and  $\bar{D} := D(\mathbf{a}^\top \otimes \mathbb{I})$ . By considering augmented inputs  $\psi(u_k)$  and outputs  $\phi(y_k)$ , (4) admits linearity in the sense that for any two input-output trajectories of (4), their linear combinations are still valid trajectories. However, as also pointed out in [19], (4) is not a standard linear model since the operator  $(\mathbf{b}^\top \otimes \mathbb{I}) \in \mathbb{R}^{n_y \times n_y q}$  is not invertible. This prohibits the use of Willems' fundamental lemma to quantify all possible input-output trajectories and provide data-driven predictions when unknown nonlinear output uncertainties exist. In addition, the assumption of having finite-dimensional basis function knowledge is restrictive and impractical for many applications.

### III. GAUSSIAN PROCESS DATA-DRIVEN PREDICTION

#### A. Gaussian Process Regression

Since the input and output nonlinearities are unknown, they are modeled as Gaussian processes with prior distributions:

$$\begin{aligned} \psi(\cdot) &\sim \mathcal{GP}(m_u(\cdot), k_u(\cdot, \cdot; \theta_u)), \\ \phi(\cdot) &\sim \mathcal{GP}(m_y(\cdot), k_y(\cdot, \cdot; \theta_y)), \end{aligned} \quad (5)$$

where  $m_u : \mathbb{R}^{n_u} \rightarrow \mathbb{R}^{n_u}$ ,  $m_y : \mathbb{R}^{n_y} \rightarrow \mathbb{R}^{n_y}$  are the mean functions,  $k_u : \mathbb{R}^{n_u} \times \mathbb{R}^{n_u} \rightarrow \mathbb{R}^{n_u}$ ,  $k_y : \mathbb{R}^{n_y} \times \mathbb{R}^{n_y} \rightarrow \mathbb{R}^{n_y}$  are the kernel/covariance functions, and  $\theta_u$  and  $\theta_y$  are hyperparameters for the kernel.

*Remark 4:* Most standard kernel structures include a scaling parameter as a hyperparameter. In our setting, as discussed in Remark 1, this scaling parameter can be fixed to 1 without loss of generality. Similarly, the mean functions  $m_u$  and  $m_y$  can also be normalized.

We are interested in jointly learning the linear mapping  $\Gamma_1, \Gamma_2$  and the nonlinearities  $\psi(\cdot)$  and  $\phi(\cdot)$ . Although the prior distribution of  $\Gamma_1, \Gamma_2$  can be derived from (3) and the Gaussian prior (5), it is dependent on  $\psi(\cdot)$  and  $\phi(\cdot)$  in a nonlinear way, and thus the Gaussianity is not preserved. Instead, we opt for directly learning  $\Gamma_1, \Gamma_2$  in a hierarchical model as will be detailed later.

*Remark 5:* When input or output nonlinearities are absent, an identity prior mean function and a zero kernel function can be selected. For example, for Hammerstein systems, we can set  $m_y(y) = y$  and  $k_y(\cdot, \cdot) = 0$ .

We first briefly summarize the standard procedure of Gaussian process regression [29]. Consider the problem of learning an unknown function  $f : \mathbb{R}^{n_\eta} \rightarrow \mathbb{R}^{n_\chi}$  from data  $(\boldsymbol{\eta}^d, \boldsymbol{\chi}^d) = (\eta_k^d, \chi_k^d)_{k=1}^M$ , where  $\chi_k^d = f(\eta_k^d) + \epsilon_k$  and  $\epsilon_k$  is zero-mean i.i.d. Gaussian with covariance  $\Sigma$ . The function  $f$  is modeled as a Gaussian process with prior mean  $m(\cdot)$ , prior covariance  $k(\cdot, \cdot; \Theta)$ , and hyperparameters  $\Theta$ , i.e.,

$$f(\cdot) \sim \mathcal{GP}(m(\cdot), k(\cdot, \cdot; \Theta)).$$

To predict  $f(\eta)$  at any query point  $\eta$ , the joint distribution of  $f(\eta)$  and  $\boldsymbol{\chi}^d$  is given by the following Gaussian distribution:

$$\begin{bmatrix} f(\eta) \\ \boldsymbol{\chi}^d \end{bmatrix} \sim \mathcal{N} \left( \begin{bmatrix} m(\eta) \\ \mathbf{m}(\boldsymbol{\eta}^d) \end{bmatrix}, \begin{bmatrix} k(\eta, \eta) & \mathbf{k}^\top(\boldsymbol{\eta}^d, \eta) \\ \mathbf{k}(\boldsymbol{\eta}^d, \eta) & K(\boldsymbol{\eta}^d, \boldsymbol{\eta}^d) + \bar{\Sigma} \end{bmatrix} \right),$$

where  $\bar{\Sigma} := \mathbb{I} \otimes \Sigma$ ,

$$\mathbf{m}(\boldsymbol{\eta}^d) := \text{col}(m(\eta_1^d), \dots, m(\eta_M^d)), \quad (6)$$

$$\mathbf{k}(\boldsymbol{\eta}^d, \eta) := \text{col}(k(\eta_1^d, \eta), \dots, k(\eta_M^d, \eta)), \quad (7)$$

$$K(\boldsymbol{\eta}^d, \boldsymbol{\eta}^d) := \begin{bmatrix} k(\eta_1^d, \eta_1^d) & k(\eta_1^d, \eta_2^d) & \dots & k(\eta_1^d, \eta_M^d) \\ k(\eta_2^d, \eta_1^d) & k(\eta_2^d, \eta_2^d) & \dots & k(\eta_2^d, \eta_M^d) \\ \vdots & \vdots & \ddots & \vdots \\ k(\eta_M^d, \eta_1^d) & k(\eta_M^d, \eta_2^d) & \dots & k(\eta_M^d, \eta_M^d) \end{bmatrix}. \quad (8)$$

This leads to the conditional probability of  $f(\eta) | \boldsymbol{\chi}^d$  as

$$f(\eta) | \boldsymbol{\chi}^d \sim \mathcal{N}(m_p(\eta), k_p(\eta)), \quad (9)$$

where

$$m_p(\eta) := m(\eta) + \mathbf{k}^\top(\boldsymbol{\eta}^d, \eta) (K + \bar{\Sigma})^{-1} (\boldsymbol{\chi}^d - \mathbf{m}(\boldsymbol{\eta}^d)), \quad (10)$$

$$k_p(\eta) := k(\eta, \eta) - \mathbf{k}^\top(\boldsymbol{\eta}^d, \eta) (K + \bar{\Sigma})^{-1} \mathbf{k}(\boldsymbol{\eta}^d, \eta), \quad (11)$$

where the dependence of  $K$  is omitted for brevity. Then,  $f(\eta)$  is predicted as the posterior mean  $m_p(\eta)$ .

The prediction is conditioned on a particular value of the hyperparameters  $\Theta$ , which is often estimated by using the maximum marginal likelihood method, also known as the empirical Bayes method, which maximizes the probability of observing  $\boldsymbol{\chi}^d$  given the observed trajectories  $\boldsymbol{\eta}^d$  and the hyperparameters  $\Theta$  by considering  $\Theta$  as deterministic variables, i.e.,

$$\Theta = \underset{\Theta}{\text{argmax}} p(\boldsymbol{\chi}^d | \boldsymbol{\eta}^d, \Theta) \quad (12)$$

$$= \underset{\Theta}{\text{argmin}} \log \det(\Lambda(\Theta)) + \delta^\top \Lambda^{-1}(\Theta) \delta, \quad (13)$$

where  $\delta := \boldsymbol{\chi}^d - \mathbf{m}(\boldsymbol{\eta}^d)$  and

$$\Lambda(\Theta) := K(\boldsymbol{\eta}^d, \boldsymbol{\eta}^d; \Theta) + \bar{\Sigma}. \quad (14)$$

#### B. Kernel Design and Posterior Prediction

For this particular data-driven prediction problem, consider the trajectory characterization equation (2). Let  $\eta = \text{col}(\mathbf{u}, \mathbf{y})$  and

$$f(\eta) = [\Gamma_1 \ \Gamma_2 \ -\mathbb{I}] \text{col}(\Psi(\mathbf{u}), \Phi(\mathbf{y}_p), \Phi(\mathbf{y}_f)), \quad (15)$$

where  $n_\eta = (n_u + n_y)L$  and  $n_\chi = n_y L'$ . We would like to train a Gaussian process model of  $f(\eta)$  by using data  $(\boldsymbol{\eta}^d, \boldsymbol{\chi}^d)$  where  $M = N - L + 1$ ,

$$\eta_k^d = \text{col}(u_k^d, \dots, u_{k+L-1}^d, y_k^d, \dots, y_{k+L-1}^d), \chi_k^d = \mathbf{0}, \quad (16)$$

$$\bar{\Sigma} = \mathbb{I} \otimes \text{cov}([\Gamma_2 \ \mathbb{I}] \mathbf{e}) = \sigma^2 (\mathbb{I} \otimes (\Gamma_2 \Gamma_2^\top + \mathbb{I})). \quad (17)$$

This is known as an implicit Gaussian process model [26].

The prior mean and covariance functions  $m(\cdot)$  and  $k(\cdot, \cdot)$  are then derived from the Gaussian process characterization of  $\psi(\cdot)$  and  $\phi(\cdot)$  in (5).

Consider two input-output trajectories  $\eta' = \text{col}(\mathbf{u}', \mathbf{y}')$  and  $\eta'' = \text{col}(\mathbf{u}'', \mathbf{y}'')$ . The mean function is given by

$$m(\eta') = [\Gamma_1 \ \Gamma_2 \ -\mathbb{I}] \text{col}(\mathbf{m}_u(\mathbf{u}'), \mathbf{m}_y(\mathbf{y}')), \quad (18)$$

where  $\mathbf{m}_u(\cdot)$ ,  $\mathbf{m}_y(\cdot)$  apply  $m_u(\cdot)$ ,  $m_y(\cdot)$  elementwise, respectively. The covariance matrix between  $\Psi(\mathbf{u}')$  and  $\Psi(\mathbf{u}'')$  is given by  $\text{cov}(\Psi(\mathbf{u}'), \Psi(\mathbf{u}'')) = \mathbf{k}_u(\mathbf{u}', \mathbf{u}'') \in \mathbb{R}^{n_u L \times n_u L}$ , and similarly  $\text{cov}(\Phi(\mathbf{y}'), \Phi(\mathbf{y}'')) = \mathbf{k}_y(\mathbf{y}', \mathbf{y}'') \in \mathbb{R}^{n_y L \times n_y L}$ , where  $\mathbf{k}_u(\cdot, \cdot)$ ,  $\mathbf{k}_y(\cdot, \cdot)$  apply  $k_u(\cdot, \cdot)$ ,  $k_y(\cdot, \cdot)$  elementwise, respectively.

Then, we have  $\text{cov}(f(\eta'), f(\eta'')) = k(\eta', \eta'')$ , where

$$k(\eta', \eta'') := [\Gamma_1 \ \Gamma_2 \ -\mathbb{I}] \begin{bmatrix} \mathbf{k}_u(\mathbf{u}', \mathbf{u}'') & \mathbf{0} \\ \mathbf{0} & \mathbf{k}_y(\mathbf{y}', \mathbf{y}'') \end{bmatrix} \begin{bmatrix} \Gamma_1^\top \\ \Gamma_2^\top \\ -\mathbb{I} \end{bmatrix}. \quad (19)$$

This completes the Gaussian process model (9) with prior mean and covariance functions (18), (19), noise model (17), and training data (16). To simplify calculation, substituting (18) and (19) into (6)-(8), after some algebraic manipulation, we have

$$\mathbf{m}(\boldsymbol{\eta}^d) = \text{vec} \left( [\Gamma_1 \ \Gamma_2 \ -\mathbb{I}] \begin{bmatrix} \mathbf{m}_u(H_u) \\ \mathbf{m}_y(H_y) \end{bmatrix} \right), \quad (20)$$

$$\mathbf{k}(\boldsymbol{\eta}^d, \boldsymbol{\eta}^d) = (\mathbb{I} \otimes [\Gamma_1 \ \Gamma_2 \ -\mathbb{I}]) \mathbf{k}_{uy}(\boldsymbol{\eta}^d, \boldsymbol{\eta}^d) \begin{bmatrix} \Gamma_1^\top \\ \Gamma_2^\top \\ -\mathbb{I} \end{bmatrix}, \quad (21)$$

$$K(\boldsymbol{\eta}^d, \boldsymbol{\eta}^d) = (\mathbb{I} \otimes [\Gamma_1 \ \Gamma_2 \ -\mathbb{I}]) K_{uy}(\boldsymbol{\eta}^d) \left( \mathbb{I} \otimes \begin{bmatrix} \Gamma_1^\top \\ \Gamma_2^\top \\ -\mathbb{I} \end{bmatrix} \right), \quad (22)$$

where  $H_u := \mathcal{H}_L(\mathbf{u}^d)$ ,  $H_y := \mathcal{H}_L(\mathbf{y}^d)$ ,

$$\mathbf{k}_{uy} := \begin{bmatrix} \mathbf{k}_u(\text{vec}(H_u), \mathbf{u}) & \mathbf{0} \\ \mathbf{0} & \mathbf{k}_y(\text{vec}(H_y), \mathbf{y}) \end{bmatrix},$$

$$K_{uy} := \begin{bmatrix} \mathbf{k}_u(\text{vec}(H_u), \text{vec}(H_u)) & \mathbf{0} \\ \mathbf{0} & \mathbf{k}_y(\text{vec}(H_y), \text{vec}(H_y)) \end{bmatrix}.$$

From (15), we have the posterior distribution

$$[\Gamma_1 \ \Gamma_2] \text{col}(\Psi(\mathbf{u}), \Phi(\mathbf{y}_p)) - \Phi(\mathbf{y}_f) \sim \mathcal{N}(m_p(\eta), k_p(\eta)),$$

whereas the true noise-free future output trajectory  $\mathbf{y}_{f,0}$  satisfies  $[\Gamma_1 \ \Gamma_2] \text{col}(\Psi(\mathbf{u}), \Phi(\mathbf{y}_p)) - \Phi(\mathbf{y}_{f,0}) = [\Gamma_2 \ \mathbf{0}] \mathbf{e}$  according to (2). Therefore, the Gaussian process model characterizes probable trajectories of (1) in the sense that for any given input trajectory  $\mathbf{u}$  and past output trajectory  $\mathbf{y}_p$ ,  $\mathbf{y}_f$  is the future output trajectory with projected prediction error  $\Phi(\mathbf{y}_{f,0}) - \Phi(\mathbf{y}_f) \sim \mathcal{N}(m_p(\eta), \hat{k}_p(\eta))$ , where  $\hat{k}_p(\eta) = k_p(\eta) + \text{cov}([\Gamma_2 \ \mathbf{0}] \mathbf{e}) = k_p(\eta) + \sigma^2 \Gamma_2 \Gamma_2^\top$ .

Different optimality criteria can be used to obtain the optimal prediction.

1) *Maximum likelihood method*: it finds the  $\mathbf{y}_f$  that maximizes the probability of observing  $f(\eta) = \mathbf{0}$  given  $\boldsymbol{\chi}^d = \mathbf{0}$ , i.e.,

$$\mathbf{y}_f = \underset{\mathbf{y}_f}{\text{argmax}} p(f(\eta) = \mathbf{0} | \boldsymbol{\chi}^d = \mathbf{0}) \quad (23)$$

$$= \underset{\mathbf{y}_f}{\text{argmin}} \log \det(k_p(\eta)) + m_p^\top(\eta) k_p^{-1}(\eta) m_p(\eta). \quad (24)$$

2) *Minimum mean-squared error predictor*:

$$\mathbf{y}_f = \underset{\mathbf{y}_f}{\text{argmin}} \text{tr} \left( \hat{k}_p(\eta) \right) + m_p^\top(\eta) m_p(\eta). \quad (25)$$

3) *Minimum-variance unbiased predictor*

$$\mathbf{y}_f = \underset{\mathbf{y}_f}{\text{argmin}} g \left( \hat{k}_p(\eta) \right) \text{ s.t. } m_p(\eta) = \mathbf{0}, \quad (26)$$

where  $g(\cdot)$  can be any optimality criteria, such as trace, determinant, or the largest eigenvalue, i.e., the A-, D-, and E- optimality criteria.

*Remark 6*: For Hammerstein systems,  $k_p(\eta)$  does not depend on  $\mathbf{y}_f$  since  $\mathbf{k}_y(\cdot, \cdot) = \mathbf{0}$  as mentioned in Remark 5. Therefore, all optimality criteria admit their minimum when  $m_p(\eta) = \mathbf{0}$ , i.e.,  $m(\eta) - \mathbf{k}^\top(\boldsymbol{\eta}^d, \eta) (K + \bar{\Sigma})^{-1} \mathbf{m}(\boldsymbol{\eta}^d) = \mathbf{0}$ . This leads to an explicit predictor by using (18):

$$\mathbf{y}_f = [\Gamma_1 \ \Gamma_2] \text{col}(\mathbf{m}_u(\mathbf{u}), \mathbf{y}_p) - \mathbf{k}^\top(\boldsymbol{\eta}^d, \eta) (K + \bar{\Sigma})^{-1} \mathbf{m}(\boldsymbol{\eta}^d).$$

### C. Hyperparameter Tuning

There are multiple hyperparameters in the posterior distribution (9) that require tuning, including kernel parameters  $\theta_u$ ,  $\theta_y$ , the noise level  $\sigma^2$ , and linear model parameters  $\Gamma_1$ ,  $\Gamma_2$ , i.e.,  $\Theta = \{\theta_u, \theta_y, \sigma^2, \Gamma_1, \Gamma_2\}$ . It is possible to directly solve (13) for the hyperparameters.

However, the hyperparameters in this problem are high-dimensional, especially since  $[\Gamma_1 \ \Gamma_2] \in \mathbb{R}^{n_y L' \times (n_u L + n_y L)}$ , which is known to induce overfitting [29]. This problem can be alleviated by selecting a suitable prior distribution for the hyperparameter, known as the hyperprior [30]. Note that  $\Gamma_1$ ,  $\Gamma_2$  correspond to the multi-step-ahead ARX parameters of  $G(q)$ . The problem of designing priors for linear model parameters has been widely studied in system identification literature (see [3] and references therein). If the state-space parameters are known, we have from [31, Equation 14]

$$\Gamma_1 =: [\Gamma_{11} \ \Gamma_{12}], \quad \Gamma_{11} = \mathcal{O}_{L'} \mathcal{P}, \quad \Gamma_{12} = \mathcal{T}_{L'}, \quad \Gamma_2 = \mathcal{O}_{L'} \mathcal{Q},$$

where

$$\mathcal{P} := \mathcal{C}_{L_0} - A^{L_0} \mathcal{O}_{L_0}^\dagger \mathcal{T}_{L_0}, \quad \mathcal{Q} := A^{L_0} \mathcal{O}_{L_0}^\dagger,$$

$$\mathcal{T}_i := \begin{bmatrix} D & & & \\ CB & D & & \\ \vdots & \vdots & \ddots & \\ CA^{i-2}B & CA^{i-3}B & \dots & D \end{bmatrix}, \quad \mathcal{O}_i := \begin{bmatrix} C \\ CA \\ \vdots \\ CA^{i-1} \end{bmatrix},$$

$$\mathcal{C}_i := [A^{i-1}B \quad \dots \quad AB \quad B].$$

Note that  $\Gamma_{12}$  has a block lower-diagonal Toeplitz structure where the last block row corresponds to the system's Markov parameters of length  $L'$ . For a stable system  $G(q)$ , a standard stable kernel design such as the TC (tune/correlated) kernel can be applied as the hyperprior of the last block row. There is no explicit structure for  $\Gamma_{11}$  and  $\Gamma_2$ . In this work, we follow the same idea in [4, Section 5.3] and model each row of  $\Gamma_{11}$  and  $\Gamma_2$  with a stable kernel indexed by the input-output lag.

For the sake of exposition, we present the case of SISO systems with  $n_u = n_y = 1$ . For MIMO systems, the same hyperprior is enforced on each input-output channel. In detail,

Gaussian hyperpriors are considered for  $\Gamma_{11}$ ,  $\Gamma_{12}$ , and  $\Gamma_2$  with zero mean and covariances:

$$\text{cov}\left((\Gamma_{12})_{i,j}, (\Gamma_{12})_{i',j'}\right) = \begin{cases} 0, & j > i \text{ or } j' > i', \\ s_{i-j, i'-j'}, & \text{otherwise.} \end{cases}$$

$$\text{cov}\left((\Gamma_{11})_{i,j}, (\Gamma_{11})_{i',j'}\right) = \begin{cases} 0, & i \neq i', \\ s_{L_0+i-j, L_0+i'-j'}, & \text{otherwise,} \end{cases}$$

$$\text{cov}\left((\Gamma_2)_{i,j}, (\Gamma_2)_{i',j'}\right) = \begin{cases} 0, & i \neq i', \\ s_{L_0+i-j, L_0+i'-j'}, & \text{otherwise,} \end{cases}$$

where  $s_{i,j}(\zeta)$  is a stable kernel parameterized by  $\zeta$ , which is sometimes known as the hyper-hyperparameters. Throughout this work, the TC kernel is used:

$$s_{i,j}^{\text{TC}}(\zeta) := \lambda \alpha^{\max(i,j)}, \quad \zeta := [\lambda \ \alpha]^\top, \quad \lambda \geq 0, \quad 0 \leq \alpha < 1.$$

The hyper-hyperparameters  $\zeta$  can be selected by cross-validation. For alternative stable kernel design, readers are referred to [3, Section 5.5].

With hyperpriors introduced for  $\Gamma_1$  and  $\Gamma_2$ , instead of the maximum marginal likelihood problem (13) which considers all hyperparameters as deterministic variables, a joint maximum-a-posteriori/maximum likelihood problem (JMAP-ML) is considered [32]:

$$\begin{aligned} \Theta &= \underset{\Theta}{\text{argmax}} p(\boldsymbol{\chi}^d | \boldsymbol{\eta}^d, \boldsymbol{\theta}, \Gamma) p(\Gamma | \zeta) \\ &= \underset{\Theta}{\text{argmin}} \log \det(\Lambda(\Theta)) + \mathbf{m}^\top(\boldsymbol{\eta}^d) \Lambda^{-1}(\Theta) \mathbf{m}(\boldsymbol{\eta}^d) + \log p(\Gamma | \zeta), \end{aligned} \quad (27)$$

where  $\boldsymbol{\theta} := \text{col}(\theta_u, \theta_y, \sigma^2)$  is considered deterministic and  $\Gamma := [\Gamma_1 \ \Gamma_2]$  admits a hyperprior.

Vectorizing all the independent elements of  $\Gamma$ , define  $\boldsymbol{\gamma} := \text{col}(\text{vec}(\Gamma_{11}^\top), \text{vec}(\Gamma_2^\top), \gamma_{12}^\top)$ , where  $\gamma_{12}$  denotes the last row of the lower-diagonal Toeplitz matrix  $\Gamma_{12}$ . Then, the hyperprior of  $\Gamma$  can be expressed as  $\boldsymbol{\gamma} | \zeta \sim \mathcal{N}(\mathbf{0}, S_\gamma)$ , where

$$S_\gamma := \text{blkdiag}(S_{L_0:1}, S_{L_0+1:2}, \dots, S_{L-1:L'}, S_{L_0:1}, S_{L_0+1:2}, \dots, S_{L-1:L'}, S_{L'-1:0}),$$

where the  $(i, j)$ -th element of  $S_{m:n} \in \mathbb{R}^{(m-n+1) \times (m-n+1)}$  is  $s_{m-i+1, m-j+1}$ . Therefore, the JMAP-ML problem (27) is equivalent to

$$\bar{\Theta} = \underset{\bar{\Theta}}{\text{argmin}} \log \det(\Lambda(\bar{\Theta})) + \mathbf{m}^\top(\boldsymbol{\eta}^d) \Lambda^{-1}(\bar{\Theta}) \mathbf{m}(\boldsymbol{\eta}^d) + \boldsymbol{\gamma}^\top S_\gamma^{-1} \boldsymbol{\gamma}, \quad (29)$$

where  $\bar{\Theta} := \{\boldsymbol{\theta}, \boldsymbol{\gamma}\}$ .

Algorithm 1 summarizes the procedure of implicit Gaussian process data-driven prediction for Hammerstein-Wiener systems.

#### D. Recovering Nonlinearities

In addition to output prediction, it could also be of interest to recover the input and output nonlinearities  $\psi(\cdot)$  and  $\phi(\cdot)$ . Note that as discussed in Remark 1, the nonlinearities can only be determined up to scaling factors.

To obtain  $\Psi(\mathbf{u})$  at any vector of query points  $\mathbf{u}$ , the joint distribution of  $\Psi(\mathbf{u})$  and  $\boldsymbol{\chi}^d$  is given by

$$\begin{bmatrix} \Psi(\mathbf{u}) \\ \boldsymbol{\chi}^d \end{bmatrix} \sim \mathcal{N} \left( \begin{bmatrix} \mathbf{m}_u(\mathbf{u}) \\ \mathbf{m}(\boldsymbol{\eta}^d) \end{bmatrix}, \begin{bmatrix} \mathbf{k}_u(\mathbf{u}, \mathbf{u}) & \boldsymbol{\kappa}_u^\top(\boldsymbol{\eta}^d, \mathbf{u}) \\ \boldsymbol{\kappa}_u(\boldsymbol{\eta}^d, \mathbf{u}) & K(\boldsymbol{\eta}^d, \boldsymbol{\eta}^d) + \bar{\Sigma} \end{bmatrix} \right),$$

---

#### Algorithm 1 Implicit Gaussian process data-driven prediction of Hammerstein-Wiener systems

---

- 1: **Given:** hyper-hyperparameters  $\zeta$ , Hankel data matrices  $H_u, H_y$
  - 2: Solve (29) for  $\bar{\Theta}$ , where  $\Lambda(\bar{\Theta})$  is given by (14), (17), (22) and  $\mathbf{m}(\boldsymbol{\eta}^d)$ ,  $S_\gamma$  are given by (20) and (28), respectively.
  - 3: Construct  $\Gamma_1, \Gamma_2$  from  $\boldsymbol{\gamma}$ .
  - 4: **Input:** Prediction condition  $\mathbf{u}, \mathbf{y}_p$
  - 5: Solve (24), (25), or (26) for  $\mathbf{y}_f$ , where  $m_p(\eta)$ ,  $k_p(\eta)$  are given by (10), (11), (17)-(22).
  - 6: **Output:** Output prediction  $\mathbf{y}_f$
- 

where, similar to the derivation in Section III-B,

$$\boldsymbol{\kappa}_u(\boldsymbol{\eta}^d, \mathbf{u}) := (\mathbb{I} \otimes \Gamma_1) \mathbf{k}_u(\text{vec}(H_u), \mathbf{u}). \quad (30)$$

Similarly, define

$$\boldsymbol{\kappa}_y(\boldsymbol{\eta}^d, \mathbf{y}) := (\mathbb{I} \otimes [\Gamma_2 \ -\mathbb{I}]) \mathbf{k}_y(\text{vec}(H_y), \mathbf{y}) \quad (31)$$

for  $\Phi(\mathbf{y})$ . This leads to the posterior distributions of  $\Psi(\mathbf{u})$  and  $\Phi(\mathbf{y})$ :

$$\begin{aligned} \Psi(\mathbf{u}) | \boldsymbol{\chi}^d &\sim \mathcal{N}(\mathbf{m}_{up}(\mathbf{u}), \mathbf{k}_{up}(\mathbf{u})), \\ \Phi(\mathbf{y}) | \boldsymbol{\chi}^d &\sim \mathcal{N}(\mathbf{m}_{yp}(\mathbf{y}), \mathbf{k}_{yp}(\mathbf{y})), \end{aligned} \quad (32)$$

where

$$\begin{aligned} \mathbf{m}_{up}(\mathbf{u}) &:= \mathbf{m}_u(\mathbf{u}) - \boldsymbol{\kappa}_u^\top(\boldsymbol{\eta}^d, \mathbf{u}) (K + \bar{\Sigma})^{-1} \mathbf{m}(\boldsymbol{\eta}^d), \\ \mathbf{k}_{up}(\mathbf{u}) &:= \mathbf{k}_u(\mathbf{u}, \mathbf{u}) - \boldsymbol{\kappa}_u^\top(\boldsymbol{\eta}^d, \mathbf{u}) (K + \bar{\Sigma})^{-1} \boldsymbol{\kappa}_u(\boldsymbol{\eta}^d, \mathbf{u}). \end{aligned}$$

and similarly for  $\mathbf{m}_{yp}(\mathbf{y})$  and  $\mathbf{k}_{yp}(\mathbf{y})$ . Then,  $\Psi(\mathbf{u})$  and  $\Phi(\mathbf{y})$  are estimated as  $\mathbf{m}_{up}(\mathbf{u})$  and  $\mathbf{m}_{yp}(\mathbf{y})$ , respectively.

#### IV. DATA-DRIVEN PREDICTIVE CONTROL WITH IMPLICIT GAUSSIAN PROCESS MODEL

This section applies preceding horizon data-driven predictive control using the implicit Gaussian process predictor described in Section III. In detail, considering the problem of tracking an output reference  $r_k$  at time  $k$ , the following expected control cost is considered at time  $k$ :

$$J_{\text{ctr}} := \|\mathbf{u}^k\|_R^2 + \mathbb{E} \left[ \|\Phi(\mathbf{y}_0^k) - \Phi(\mathbf{r}^k)\|_Q^2 \right], \quad (33)$$

where  $R \in \mathbb{R}^{n_u L' \times n_u L'}$ ,  $Q \in \mathbb{R}^{n_y L' \times n_y L'}$  are the input and the output cost matrices, respectively, and  $\mathbf{r}^k := \text{col}(r_k, \dots, r_{k+L'-1})$ ,  $\mathbf{u}^k := \text{col}(u_k, \dots, u_{k+L'-1})$ ,  $\mathbf{y}_0^k := \text{col}(y_{k,0}, \dots, y_{k+L'-1,0})$  are the reference, input, and true output trajectories at time  $k$ , respectively. In addition, we also consider input constraints  $\mathbf{u}^k \in \mathcal{U}_k$  and linear output constraints  $H \mathbf{y}_0^k \leq q$ , where  $H \in \mathbb{R}^{n_c \times n_y L'}$  and  $q \in \mathbb{R}^{n_c}$ . Since the prediction error is unbounded, the output constraint can only be enforced with high probability  $p$  as a chance constraint  $\Pr(H \mathbf{y}_0^k \leq q) \geq p$ .

In this section, the following assumption is considered.

*Assumption 2:* The output nonlinearity  $\phi^{-1}(\cdot)$  is Lipschitz continuous with  $\|\phi^{-1}(\bar{y}_1) - \phi^{-1}(\bar{y}_2)\|_2 \leq M \|\bar{y}_1 - \bar{y}_2\|_2$ , where  $M$  is the Lipschitz constant.

As discussed in Section III, the distribution of  $\Phi(\mathbf{y}_0^k)$  is given by

$$\Phi(\mathbf{y}_0^k) \sim \mathcal{N}\left(\Phi(\mathbf{y}^k) + m_p(\eta^k), \hat{k}_p(\eta^k)\right), \quad (34)$$

where  $\mathbf{y}^k$  is the output prediction and

$$\eta^k := \text{col}(u_{k-L_0}, \dots, u_{k-1}, \mathbf{u}^k, y_{k-L_0}, \dots, y_{k-1}, \mathbf{y}^k).$$

Then, we have the following lemma.

*Lemma 2:* Under Assumptions 1 and 2, the chance constraint  $\Pr(H\mathbf{y}_0^k \leq q) \geq p$  is guaranteed by

$$H\mathbf{y}^k \leq q - c_p \sqrt{\text{diag}(HH^\top)}, \quad (35)$$

where  $c_p := M \left( \sqrt{\mu(p)\sigma_p(\eta^k)} + \|m_p(\eta^k)\|_2 \right)$ ,  $\sigma_p(\eta^k)$  is the largest eigenvalue of  $\hat{k}_p(\eta^k)$  and  $\mu(\cdot)$  is the quantile function of the  $\chi^2$ -distribution with  $n_y L'$  degrees of freedom.

*Proof:* We have

$$\Pr\left(\|\Phi(\mathbf{y}_0^k) - \Phi(\mathbf{y}^k) - m_p(\eta^k)\|_{\hat{k}_p^{-1}(\eta^k)}^2 \leq \mu(p)\right) = p,$$

since  $\|\Phi(\mathbf{y}_0^k) - \Phi(\mathbf{y}^k) - m_p(\eta^k)\|_{\hat{k}_p^{-1}(\eta^k)}^2$  follows a  $\chi^2$ -distribution with  $n_y L'$  degrees of freedom. According to Assumptions 1.3) and 2, we have

$$\begin{aligned} & \|\Phi(\mathbf{y}_0^k) - \Phi(\mathbf{y}^k) - m_p(\eta^k)\|_{\hat{k}_p^{-1}(\eta^k)} \\ & \geq \frac{1}{\sqrt{\sigma_p(\eta^k)}} \|\Phi(\mathbf{y}_0^k) - \Phi(\mathbf{y}^k) - m_p(\eta^k)\|_2 \\ & \geq \frac{1}{\sqrt{\sigma_p(\eta^k)}} \left( \|\Phi(\mathbf{y}_0^k) - \Phi(\mathbf{y}^k)\|_2 - \|m_p(\eta^k)\|_2 \right) \\ & \geq \frac{1}{M\sqrt{\sigma_p(\eta^k)}} \|\mathbf{y}_0^k - \mathbf{y}^k\|_2 - \frac{1}{\sqrt{\sigma_p(\eta^k)}} \|m_p(\eta^k)\|_2. \end{aligned}$$

This leads to  $\Pr(\|\mathbf{y}_0^k - \mathbf{y}^k\|_2 \leq c_p) \geq p$ . If  $\|\mathbf{y}_0^k - \mathbf{y}^k\|_2 \leq c_p$ , according to [33, Theorem 2.3],  $H\mathbf{y}_0^k \leq q$  is guaranteed by

$$h_i^\top \mathbf{y}^k \leq q_i - \tau_V(h_i), \quad i = 1, \dots, n_c, \quad (36)$$

where  $H =: \text{col}(h_1^\top, \dots, h_{n_c}^\top)$ ,  $q =: \text{col}(q_1, \dots, q_{n_c})$ , and  $\tau_V(h_i) = c_p \sqrt{h_i^\top h_i}$  denotes the support function of set  $V := \{\mathbf{e} \mid \|\mathbf{e}\|_2 \leq c_p\}$ . Aggregating (36) for all  $i$  directly leads to the lemma. ■

From the distribution (34), the expected control cost can be calculated as

$$J_{\text{cur}} = \|\mathbf{u}^k\|_R^2 + \|\Phi(\mathbf{y}^k) + m_p(\eta^k) - \Phi(\mathbf{r}^k)\|_Q^2 + \text{tr}\left(Q\hat{k}_p(\eta^k)\right).$$

Instead of providing an output prediction for a particular input, the control problem optimizes  $\mathbf{u}^k$  and  $\mathbf{y}^k$  at the same time by penalizing a combination of the nominal tracking error  $\|\Phi(\mathbf{y}^k) + m_p(\eta^k) - \Phi(\mathbf{r}^k)\|_Q^2$  and the prediction error  $\text{tr}\left(Q\hat{k}_p(\eta^k)\right)$ . This avoids applying Algorithm 1 directly in the control problem, i.e., solving (24), (25), or (26) as an inner problem. Since the output nonlinearity  $\Phi(\cdot)$  is not known exactly,  $\Phi(\mathbf{y}^k)$  and  $\Phi(\mathbf{r}^k)$  are replaced by their posterior means  $\mathbf{m}_{yp}(\mathbf{y}^k)$  and  $\mathbf{m}_{yp}(\mathbf{r}^k)$  with certainty equivalence.

To sum up, the following optimization problem is solved at time  $k$ :

$$\begin{aligned} & \min_{\mathbf{u}^k, \mathbf{y}^k} \|\mathbf{u}^k\|_R^2 + \|\mathbf{m}_{yp}(\mathbf{y}^k) + m_p(\eta^k) - \mathbf{m}_{yp}(\mathbf{r}^k)\|_Q^2 + \text{tr}\left(Q\hat{k}_p(\eta^k)\right) \\ & \text{s.t. } \mathbf{u}^k \in \mathcal{U}_k, H\mathbf{y}^k \leq q - c_p \sqrt{\text{diag}(HH^\top)}. \end{aligned} \quad (37)$$

Then, the first entry in the optimal input sequence is applied to the system and the noisy output  $y_k$  is measured.

## V. NUMERICAL EXAMPLES

This section demonstrates the performance of the proposed data-driven predictor (Algorithm 1) and controller (37).<sup>1</sup>

Consider Hammerstein-Wiener systems with input and output nonlinearities  $\psi(u) = u + \sin(u)$ ,  $\phi^{-1}(\bar{y}) = \bar{y} + \sin(\bar{y})$  and random single-input, single-output second-order systems for the linear part  $G(q)$ , generated by the MATLAB function `drss` and normalized to have an  $\mathcal{H}_2$ -norm of 10. The output nonlinearity satisfies Assumption 2 with  $M = 2$ . The following parameters are used:  $L_0 = 2$ ,  $N = 100$ ,  $\sigma = 0.01$ . Unit Gaussian inputs are used for both training and testing. The hyper-hyperparameters  $\zeta = [\lambda \alpha]^\top$  are selected by cross-validation with grid  $\lambda \in \{0.25, 0.5, 1, 2, 4\}$ ,  $\alpha \in \{0.5, 0.6, 0.7, 0.8, 0.9\}$ . The squared exponential kernel is used for  $k_u(\cdot, \cdot)$  and  $k_y(\cdot, \cdot)$ , i.e.,  $k_u(u', u''; l_u) = \exp\left(-\frac{(u' - u'')^2}{2l_u^2}\right)$  with hyperparameter  $l_u$ , and similarly for  $k_y(y', y''; l_y)$ . Note that the scaling factor is omitted as discussed in Remark 4. The prior mean functions are selected as identity, i.e.,  $m_u(u) = u$ ,  $m_y(y) = y$ . The minimum mean-squared error objective (25) is used to obtain explicit predictions in Algorithm 1 and solved using the MATLAB function `particleswarm` with a particle swarm solver. The other optimization problems (29) and (37) are solved using the MATLAB function `fmincon` with the sequential quadratic programming algorithm.

The proposed implicit Gaussian process model is benchmarked against a black-box Gaussian process model of

$$y_{f,l} \sim \mathcal{N}\left(m_{\text{bb},l}(\text{col}(\mathbf{u}, \mathbf{y}_p)), \sigma_{\text{bb},l}^2(\text{col}(\mathbf{u}, \mathbf{y}_p))\right),$$

where  $l = 1, \dots, L'$  and  $m_{\text{bb},l}(\cdot)$ ,  $\sigma_{\text{bb},l}(\cdot)$  are the posterior output prediction and standard deviation of the  $l$ -step-ahead predictor, respectively. The model is trained using default settings of the MATLAB function `fitrgp`. We also compare a linear predictor based on Willems' fundamental lemma, neglecting the nonlinearities:  $\mathbf{y}_f = H_{yf} \text{col}(H_u, H_{yp})^\dagger \text{col}(\mathbf{u}, \mathbf{y}_p)$ , where  $H_y =: \text{col}(H_{yp}, H_{yf})$ ,  $H_{yp} \in \mathbb{R}^{n_y L_0 \times M}$ , and  $H_{yf} \in \mathbb{R}^{n_y L' \times M}$ .

For demonstrative purposes, we first consider the case where  $L' = 1$ . Figure 2 demonstrates the prediction accuracy of the predictors on a test data set. The recovered input and output nonlinear functions are plotted in Figure 3 by applying (32) to a linear grid of query points between  $-\pi$  and  $\pi$ . It can be seen from Figure 2 that Algorithm 1 obtains very accurate predictions and performs much better than the black-box Gaussian process model and the linear predictor. The black-box predictions are similar to the linear ones, indicating that the black-box Gaussian process model does not capture the nonlinearities well. As can be seen from Figure 3, the shapes of the nonlinearities are captured correctly. There is a discrepancy of  $\psi(u)$  in terms of the scaling, which is expected since only the normalized nonlinearities are recovered.

Then, multi-step-ahead predictors with  $L' = 4$  are considered by conducting 50 Monte Carlo simulations. At each time

<sup>1</sup>The codes are available at <https://doi.org/10.25835/0ahxlrtrw>.

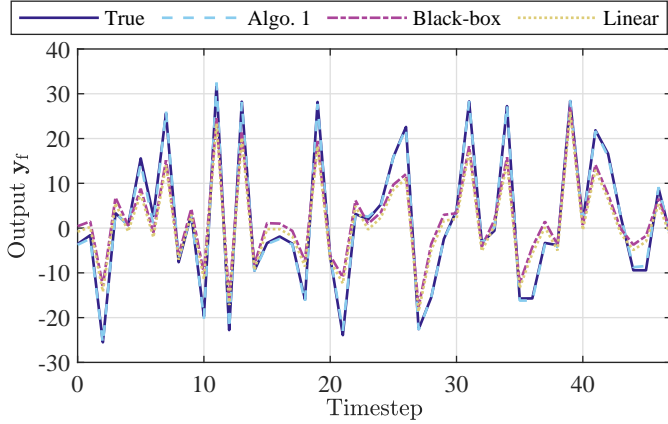


Fig. 2. Comparison of data-driven prediction with different predictors.

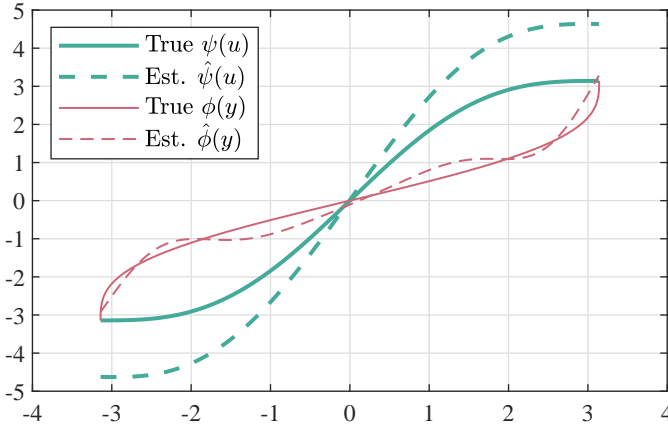


Fig. 3. Estimation of input and output nonlinear functions  $\psi(u)$  and  $\phi(y)$ .

$k$ ,  $l$ -step-ahead prediction accuracy is evaluated quantitatively on a test data set by comparing the  $l$ -step-ahead prediction at time  $k$  with the true output at time  $(k+l)$ ,  $l = 1, 2, 3, 4$ . In addition to the predictors presented before, we also consider the implicit Gaussian process model with hyperparameters estimated without the hyperprior, i.e.,  $S_\gamma^{-1} = \mathbf{0}$  in (29). The median root-mean-squared prediction errors are shown in Table I. Similar to one-step-ahead prediction, our proposed algorithm achieves the smallest prediction errors across the horizon, with an overall error reduction of 40% and 38% compared to the black-box Gaussian process model and the linear predictor, respectively. On the other hand, a significant prediction error is observed for Algorithm 1 without using the hyperprior in hyperparameter estimation. This indicates that the proposed method would fail without the hyperprior and validates the effectiveness of the proposed JMAP-ML scheme for hyperparameter estimation.

Finally, the data-driven predictive control algorithm (37) is applied where we consider the following second-order system for  $G(q)$ :

$$G(q) = \frac{10q}{q^2 + 0.24q + 0.36}$$

with prediction horizon  $L' = 4$ . We have also implemented receding horizon control for the black-box and the linear

TABLE I  
MEDIAN ROOT-MEAN-SQUARED PREDICTION ERRORS OF DIFFERENT PREDICTORS WITH  $L' = 4$

$l$	1	2	3	4
<b>Algorithm 1</b>	3.532	3.742	4.171	3.983
<b>Algorithm 1 w/o hyperprior</b>	17.074	17.101	17.281	18.067
<b>Black-box model</b>	6.062	6.439	6.528	6.708
<b>Linear predictor</b>	5.965	6.317	6.395	6.398

predictors. For the black-box Gaussian process model, the following optimization problem is solved at time  $k$ :

$$\begin{aligned} \min_{\mathbf{u}^k, \mathbf{y}^k} & \quad \|\mathbf{u}^k\|_R^2 + \|\mathbf{y}^k - \mathbf{r}^k\|_Q^2 + \text{diag}(Q)^\top \boldsymbol{\sigma}_{\text{bb}}^2(\xi^k) \\ \text{s.t.} & \quad \mathbf{y}^k = \mathbf{m}_{\text{bb}}(\xi^k), \quad \mathbf{u}^k \in \mathcal{U}_k, \\ & \quad H\mathbf{y}^k \leq q - \bar{\sigma}_{\text{bb}}(\xi^k) \sqrt{\mu(p) \text{diag}(HH^\top)}, \end{aligned}$$

where  $\xi^k = \text{col}(u_{k-L_0}, \dots, u_{k-1}, \mathbf{u}^k, y_{k-L_0}, \dots, y_{k-1})$  and  $\bar{\sigma}_{\text{bb}}(\xi^k)$  denotes the largest element of  $\boldsymbol{\sigma}_{\text{bb}}(\xi^k)$ . The derivation is similar to Section IV. For the linear predictor, we apply subspace predictive control [28] with certainty equivalence.

A sinusoidal output reference with lower and upper bound constraints is considered. No input constraints are enforced, i.e.,  $\mathcal{U}_k = \mathbb{R}^{L'}$ . The following parameters are used:  $M = 2$ ,  $p = 0.7$ ,  $Q = R = \mathbb{I}$ . To avoid infeasibilities, the tightened output constraints are implemented as soft constraints with a penalty weight of 100.

The closed-loop output trajectories are plotted in Figure 4. The results demonstrate that only the proposed control algorithm (37) is able to track the reference closely within the output bounds. The black-box Gaussian process model cannot provide any reasonable control due to its large posterior standard deviation leading to severe constraint violation throughout the simulation. The prediction performance of the proposed algorithm is further analyzed in Figure 5. It can be seen that the output predictions are very close to the true output trajectory and the posterior standard deviation provides a good estimate of the prediction error with the true trajectory staying within the one standard deviation range from the predictions for most of the time.

## VI. CONCLUSIONS

This work presents data-driven prediction and control algorithms of Hammerstein-Wiener systems by implicit Gaussian process regression. By formulating the predictor as an implicit function, a Gaussian process model is obtained by deriving kernel functions with Gaussian process priors for nonlinearities. A stable spline hyperprior is used to estimate linear model parameters as hyperparameters. Applied to receding horizon control, the algorithm minimizes the expected control cost and complies with output chance constraints. Validation through numerical examples demonstrates improved performance over the black-box Gaussian process method.

One drawback of the proposed approach is its high computational complexity due to a high number of hyperparameters and complex kernel design. Future work may discuss optimization algorithms for solving the hyperparameter tuning

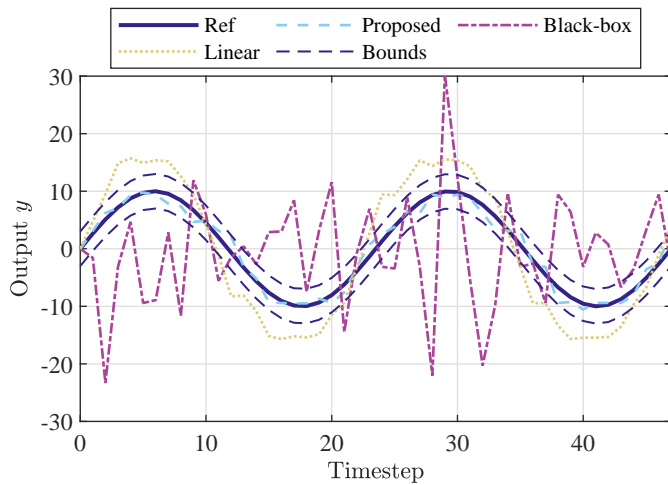


Fig. 4. Closed-loop output trajectories with different data-driven predictive controllers.

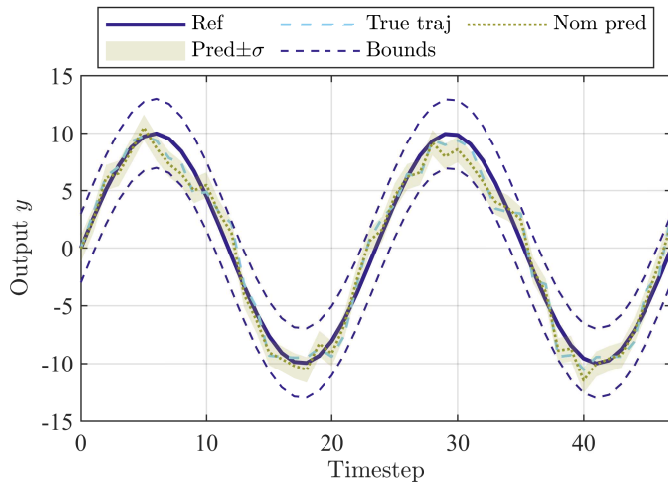


Fig. 5. Prediction accuracy and error bounds of the proposed control algorithm.

problem. Closed-loop guarantees for the receding horizon control algorithm can also be investigated.

## REFERENCES

- [1] F. Giri and E.-W. Bai, *Block-oriented nonlinear system identification*. Springer, 2010.
- [2] M. Lazar, “Basis-functions nonlinear data-enabled predictive control: Consistent and computationally efficient formulations,” in *European Control Conference (ECC)*, 2024, p. 888–893.
- [3] G. Pillonetto, T. Chen, A. Chiuso, G. De Nicolao, and L. Ljung, *Regularized system identification: learning dynamic models from data*. Springer, 2022.
- [4] G. Pillonetto, F. Dinuzzo, T. Chen, G. De Nicolao, and L. Ljung, “Kernel methods in system identification, machine learning and function estimation: A survey,” *Automatica*, vol. 50, no. 3, p. 657–682, 2014.
- [5] G. Pillonetto, M. H. Quang, and A. Chiuso, “A new kernel-based approach for nonlinear system identification,” *IEEE Transactions on Automatic Control*, vol. 56, no. 12, p. 2825–2840, 2011.
- [6] R. S. Risuleo, G. Bottegal, and H. Hjalmarsson, “A nonparametric kernel-based approach to Hammerstein system identification,” *Automatica*, vol. 85, p. 234–247, 2017.
- [7] R. S. Risuleo, F. Lindsten, and H. Hjalmarsson, “Bayesian nonparametric identification of Wiener systems,” *Automatica*, vol. 108, p. 108480, 2019.
- [8] E. J. Cross, T. J. Rogers, D. J. Pitchforth, S. J. Gibson, S. Zhang, and M. R. Jones, “A spectrum of physics-informed Gaussian processes for regression in engineering,” *Data-Centric Engineering*, vol. 5, 2024.
- [9] L. Hewing, J. Kabzan, and M. N. Zeilinger, “Cautious model predictive control using Gaussian process regression,” *IEEE Transactions on Control Systems Technology*, vol. 28, no. 6, p. 2736–2743, 2020.
- [10] E. Bradford, L. Imsland, D. Zhang, and E. A. del Rio Chanona, “Stochastic data-driven model predictive control using Gaussian processes,” *Computers & Chemical Engineering*, vol. 139, p. 106844, 2020.
- [11] M. Maiworm, D. Limon, and R. Findeisen, “Online learning-based model predictive control with Gaussian process models and stability guarantees,” *International Journal of Robust and Nonlinear Control*, vol. 31, no. 18, p. 8785–8812, 2021.
- [12] J. C. Willems, P. Rapisarda, I. Markovskiy, and B. L. M. De Moor, “A note on persistency of excitation,” *Systems & Control Letters*, vol. 54, no. 4, pp. 325–329, 2005.
- [13] I. Markovskiy and P. Rapisarda, “Data-driven simulation and control,” *International Journal of Control*, vol. 81, no. 12, pp. 1946–1959, 2008.
- [14] J. Coulson, J. Lygeros, and F. Dorfler, “Distributionally robust chance constrained data-enabled predictive control,” *IEEE Transactions on Automatic Control*, vol. 67, no. 7, p. 3289–3304, 2022.
- [15] J. Berberich, J. Köhler, M. A. Müller, and F. Allgöwer, “Data-driven model predictive control with stability and robustness guarantees,” *IEEE Transactions on Automatic Control*, vol. 66, no. 4, pp. 1702–1717, 2021.
- [16] M. Yin, A. Iannelli, and R. S. Smith, “Maximum likelihood estimation in data-driven modeling and control,” *IEEE Transactions on Automatic Control*, vol. 68, no. 1, p. 317–328, 2023.
- [17] V. Breschi, A. Chiuso, and S. Formentin, “Data-driven predictive control in a stochastic setting: a unified framework,” *Automatica*, vol. 152, p. 110961, 2023.
- [18] M. Alsalti, M. Barkey, V. G. Lopez, and M. A. Müller, “Robust and efficient data-driven predictive control,” *arXiv preprint arXiv:2409.18867*, 2024.
- [19] J. Berberich and F. Allgöwer, “A trajectory-based framework for data-driven system analysis and control,” in *2020 European Control Conference (ECC)*, 2020.
- [20] O. Molodchyk and T. Faulwasser, “Exploring the links between the fundamental lemma and kernel regression,” *IEEE Control Systems Letters*, vol. 8, p. 2045–2050, 2024.
- [21] J. G. Rueda-Escobedo and J. Schiffer, “Data-driven internal model control of second-order discrete Volterra systems,” in *IEEE Conference on Decision and Control (CDC)*, 2020.
- [22] M. Alsalti, V. G. Lopez, J. Berberich, F. Allgöwer, and M. A. Müller, “Data-based control of feedback linearizable systems,” *IEEE Transactions on Automatic Control*, vol. 68, no. 11, p. 7014–7021, 2023.
- [23] Z. Yuan and J. Cortes, “Data-driven optimal control of bilinear systems,” *IEEE Control Systems Letters*, vol. 6, p. 2479–2484, 2022.
- [24] I. Markovskiy, “Data-driven simulation of generalized bilinear systems via linear time-invariant embedding,” *IEEE Transactions on Automatic Control*, vol. 68, no. 2, p. 1101–1106, 2023.
- [25] X. Shang, J. Cortés, and Y. Zheng, “Willems’ fundamental lemma for nonlinear systems with Koopman linear embedding,” *arXiv preprint arXiv:2409.16389*, 2024.
- [26] W. Martens, Y. Poffet, P. R. Soria, R. Fitch, and S. Sukkarieh, “Geometric priors for Gaussian process implicit surfaces,” *IEEE Robotics and Automation Letters*, vol. 2, no. 2, p. 373–380, 2017.
- [27] W. Favoreel, B. D. Moor, and M. Gevers, “SPC: Subspace predictive control,” *IFAC Proceedings Volumes*, vol. 32, no. 2, pp. 4004–4009, 1999.
- [28] F. Fiedler and S. Lucia, “On the relationship between data-enabled predictive control and subspace predictive control,” in *European Control Conference (ECC)*, 2021, pp. 222–229.
- [29] C. E. Rasmussen and C. K. I. Williams, *Gaussian Processes for Machine Learning*. The MIT Press, 2005.
- [30] M. Khosravi, M. Yin, A. Iannelli, A. Parsi, and R. S. Smith, “Low-complexity identification by sparse hyperparameter estimation,” *IFAC-PapersOnLine*, vol. 53, no. 2, p. 412–417, 2020.
- [31] A. Iannelli, M. Yin, and R. S. Smith, “Design of input for data-driven simulation with Hankel and page matrices,” in *2021 60th IEEE Conference on Decision and Control (CDC)*, 2021.
- [32] A. Yeredor, “The joint MAP-ML criterion and its relation to ML and to extended least-squares,” *IEEE Transactions on Signal Processing*, vol. 48, no. 12, p. 3484–3492, 2000.
- [33] I. Kolmanovskiy and E. G. Gilbert, “Theory and computation of disturbance invariant sets for discrete-time linear systems,” *Mathematical problems in engineering*, vol. 4, no. 4, pp. 317–367, 1998.